Seismic Design of Concrete-Filled Circular Steel Bridge Piers

Michel Bruneau, M.ASCE,[1] and Julia Marson[2]

Abstract: The adequacy of the existing design provisions for concrete-filled steel pipes subjected to axial forces and flexure is reviewed by comparing the strengths predicted by the CAN/CSA-S16.1-M94, AISC LRFD 1994, and the Eurocode 4 1994 codes and standards against experimental data from a number of investigators. New proposed design equations are then developed, in a format compatible with North American practice. The new equations, based on a simple plasticity model calibrated using experimental data, are shown to provide improved correlation between predicted strength and experimental data. This paper provides information and data in support of the proposed design equations, which have already been implemented in the 2001 edition of the CSA-S16-01 ''limit state design of steel structures'' (CSA 2001) and in the ''Recommended LRFD Guidelines for the Seismic Design of Highway Bridges'' (MCEER/ATC 2003).

DOI: 10.1061/(ASCE)1084-0702(2004)9:1(24)

CE Database subject headings: Bridge piers; Composite columns; Cyclic tests; Seismic response; Footings; Design criteria.

Introduction

Filling a steel pipe with unreinforced concrete can remarkably increase its strength and ductility to resist seismically induced flexure. The steel shell provides some confinement for the concrete, which in turn delays local buckling of the steel, allowing effective composite action to develop. There are a number of national codes and standards that provide equations for the design of concrete-filled steel hollow sections. However, there is no unique method to calculate compressive or moment resistance.

In the United States, the first code clauses for composite column construction of the type considered here were introduced in 1963 by the American Concrete Institute ''Building Code Requirements for Reinforced Concrete'' (ACI 1963) and later in 1986 by the first edition of the American Institute of Steel Construction ''load and resistance factor design (LRFD) specifications for structural steel buildings'' (AISC 1986). In North America some newer buildings with composite columns have been designed using these procedures (Viest et al. 1997). When such designs were accomplished prior to the availability of codified rules, they followed fundamental engineering principles and presumably some measure of conservatism. In Canada, requirements for the design of such members exist in the CAN/CSA-S16.1-M94 ''Limit States Design of Steel Structures'' (CSA 1994).

With respect to bridges, the American Association of State Highway and Transportation Officials LRFD provisions (AASHTO 1994) introduced design equations for composite compression members similar to those proposed by AISC, but without the restrictions on material properties or cross-section sizes specified by the AISC. In Canada, composite columns were not addressed by the 1988 edition of the CSA standard for the design of highway bridges CAN/CSA-S6-88 (CSA 1988), nor by the 1991 edition of the Ontario highway bridge design code (MTO 1991).

In this paper, the adequacy of the design provisions of the CAN/CSA-S16.1-M94 (CSA 1994) AISC LRFD (1994), and the Eurocode 4 1994 codes and standards are reviewed by comparing their predicted column strength with experimental data from a number of investigators. Then, experimental results reported in Marson and Bruneau (2004) are used to develop improved design equations for concrete-filled steel columns subjected to combined axial and flexural loading. The proposed equations are subsequently compared against the results predicted by the same three codes and standards considered for a broader set of experimental data.

Note that although proper terminology for the CAN/CSA-S16.1-M94 is a ''standard,'' and for the AISC LRFD (1994) is ''specifications,'' all documents are called ''codes'' here, inferring that these documents are referenced by other enforceable codes, but also to keep the following text unburdened by such subtle differences. Likewise, ''pipe'' and ''tube'' will be used interchangeably, but all refer to a circular hollow section in the context of this paper. Also note that the code equations used for the comparisons referenced throughout the paper are briefly summarized in the Appendix (space constraints preclude a detailed presentation), and that no safety factors were used in any of the comparisons made using code-based strength predictions (in other words, all ϕ factors were taken as 1.0 for the purpose of comparisons).

Code Comparisons of Axial Resistance with Previous Research

A review of 120 tests on axially loaded columns (P_f) by past researchers, along with the corresponding calculated axial resistance for each respective code equation (P_r), and the ratio of the experimental to theoretical axial resistance (P_f/P_r) was conducted by Marson and Bruneau (2000). It was found that the

[1]Director, MCEER, Professor, Dept. of CSEE, Univ. at Buffalo, Buffalo, NY 14260. E-mail: bruneau@mceermail.buffalo.edu

[2]Project Engineer, Harmer Podolak Engineering, 221-39 Robertson Rd., Nepean ON, Canada K2H 8R2.

Note. Discussion open until June 1, 2004. Separate discussions must be submitted for individual papers. To extend the closing date by one month, a written request must be filed with the ASCE Managing Editor. The manuscript for this paper was submitted for review and possible publication on June 11, 2002; approved on June 24, 2003. This paper is part of the ***Journal of Bridge Engineering***, Vol. 9, No. 1, January 1, 2004. ©ASCE, ISSN 1084-0702/2004/1-24–34/$18.00.

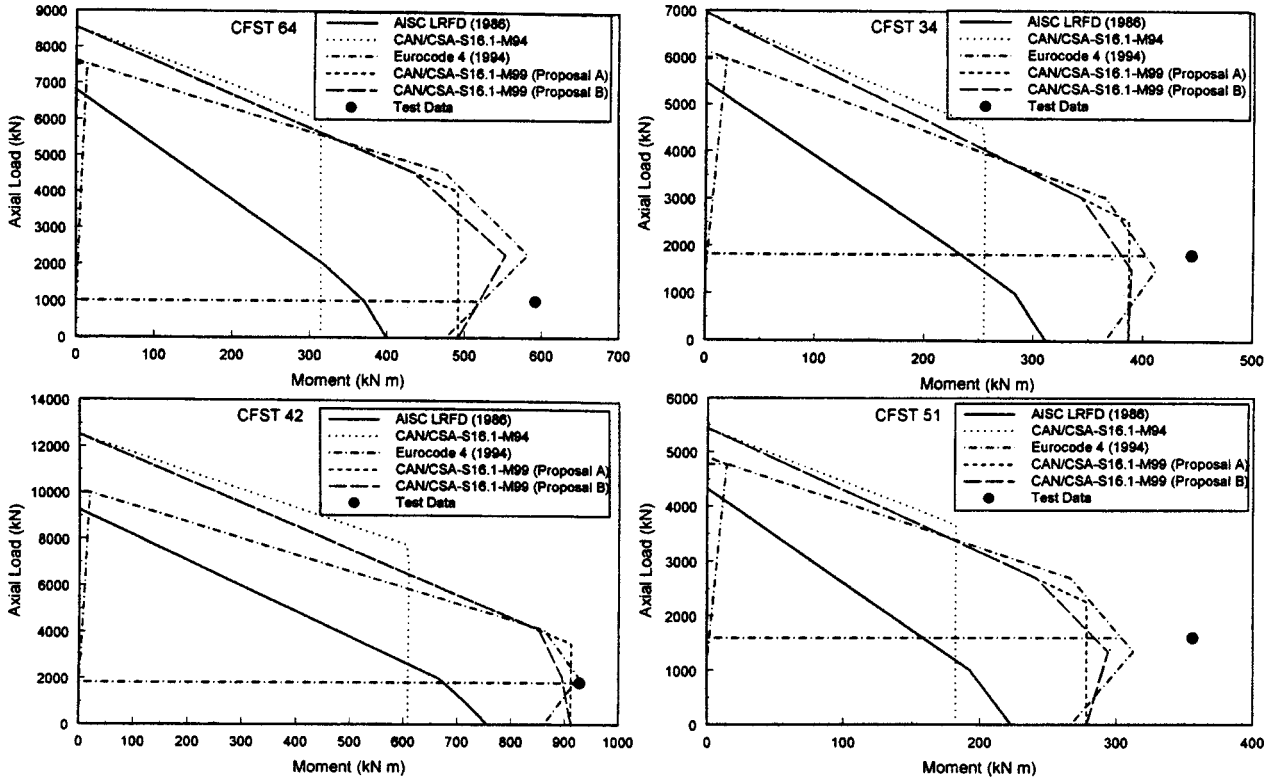

Fig. 1. Interaction diagrams per various approaches for specimens CFST 64, 51, 42, and 34

average ratio of experimental-to-theoretical axial load capacity for the entire data set considered were closest to unity for the CAN/CSA-S16.1-M94 and the Eurocode 4 1994, with values of 1.14 and 1.13, respectively, with corresponding standard deviations of 0.24 and 0.22. In spite of these close averages, the Canadian code predicted strengths up to 18% greater and 16% lower than those from the European code for different combinations of characterizing parameters. Both of these codes consider the effect of concrete confinement in circular tubes but do it in significantly different ways, which partly accounts for the differences observed for individual results. The experimental to theoretical axial resistance ratio calculated by the AISC LRFD (1994) was, on average, 1.26. This ratio is larger than obtained using the other two codes. This code does not allow for much increase in concrete strength due to confinement when compared to the previous two other codes.

Comparison of Beam-Column Capacities with Results for Specimens

Interaction curves were developed using the code procedures outlined in the Appendix for the four specimens tested by Marson and Bruneau (2004). Fig. 1 shows these curves and Table 1 summarizes the theoretical and tested moment resistance for the four columns studied. These graphs and table show the benefits and disadvantages of the three codes. The interaction curves labeled CAN/CSA-S16.1-M99 (proposal A) are described later in this paper. The curves CAN/CSA-S16.1-M99 (proposal B) are described in Marson and Bruneau (2000) but not presented here due to space constraints. [Proposal B was constructed on the basis that a concrete-filled tube can have a flexural strength at small axial forces greater than the maximum moment capacity of a section with no axial load applied, and provided equations to construct an

Table 1. Experiment to Calculated Strength Ratios for Specimens Tested by Marson and Bruneau (2002)

	CFST 64 $P = 1000$ kN		CFST 34 $P = 1820$ kN		CFST 42 $P = 1820$ kN		CFST 51 $P = 1600$ kN	
Code	Strength (kN m)	M_f/M_r	Strength (kN m)	M_f/M_r	Strength (kN m)	M_f/M_r	Strength (kN m)	M_f/M_r
Test data	591		444		928		356	
AISC LRFD (1994)	362	1.64	234	1.90	681	1.36	158	2.25
CAN/S16.1-M94	314	1.88	255	1.74	608	1.53	182	1.95
Eurocode 4 (1994)	522	1.33	402	1.10	918	1.01	304	1.17
CAN/S16.1-M99 (proposal A)	492	1.20	387	1.15	911	1.02	278	1.28
CAN/S16.1-M99 (proposal B)	519	1.14	380	1.17	897	1.04	284	1.25

interaction diagram represented by a polygon with three straight lines (similar to the concept incorporated into the Eurocode 4 1994), but with the effect of column slenderness addressed in a manner compatible with North American practice. While the advantage of proposal B over proposal A is the ability to predict greater moment capacity when a beam column is subjected to low axial forces, particularly for members of low slenderness, it was found that the enhanced accuracy of proposal B over proposal A was marginal and insufficient to justify its added complexity.] Note that the Eurocode 4 moment resistance at a given axial force level is the length of the horizontal line ranging from the strength interaction curve on the right and the diagonal line on the left side of the graph.

For all four of the specimens tested here, the best prediction of maximum moment is given by the Eurocode, with an average experimental to calculated moment resistance value of 1.15. That interaction curve is derived somewhat following the principles of an axial force-moment interaction diagram for reinforced concrete which explains its particular shape. The AISC LRFD bilinear interaction curve predicts smaller axial and flexural strengths than the Eurocode, underestimating the strength of the four specimens by 1.79 on average. CAN/CSA-S16.1-M94 also predicted similarly conservative values of maximum moment resistance (with average ratio of experimental to calculated strengths of 1.77). These low values from the Canadian code can be explained by the peculiar shape of the interaction curve shown in the figures. This results from the fact that, once the value of $C_f - \tau' C_r'$ in Eq. (31) becomes less than zero, the axial force—moment interaction curve is simply the moment resistance of the steel section acting alone (i.e., noncomposite). Therefore, at the point that $C_f - \tau' C_r' \leq 0$ the moment resistance is constant for all values of C_f below this axial force. This truncates the interaction curve in the manner shown in the figures, such that for specimens with low applied axial forces, the moment capacity of the composite section is grossly underestimated, as seen for all tested specimens.

Note that while a large underestimate of actual column strength by a design equation may be perceived as conservative in some applications, in seismic design where structural elements adjacent to yielding bridge piers must be designed as capacity protected (MCEER/ATC 2003), inaccurate estimate of the pier capacity could result in unintended undesirable damage to the nonductile structural elements that should have otherwise been capacity protected.

Comparison with Previous Research Data

Table 2 lists data from previous research on circular concrete-filled steel tube columns subjected to both axial force and flexure, along with their moment capacity calculated by code (Furlong 1967; Knowles and Park 1969; Prion and Boehme 1994; Alfawakiri 1997; Marson 1999). Results are segregated in terms of D/t ranges (corresponding to CISC classes described in Marson and Bruneau 2004). The average experimental-to-theoretical flexural strength (at the applied axial load) for all specimens considered is 3.90 with a standard deviation of 4.20 when calculated per the AISC LRFD provisions, 1.79 with a standard deviation of 0.64 per the CAN/CSA-S16.1-M94, and 1.10 with a standard deviation of 0.32 per Eurocode 4 1994.

Results are graphically summarized in Fig. 2. Vertical lines in Fig. 2 represent the limits for classes 1, 2, 3, and 4, as well as a special class 4 limit for concrete-filled steel tubes ($D/t \leq 28000/F_y$), as defined by CAN/CSA-S16.1-M94. Fig. 3 illustrates the effect of axial load ratio to the ratio of experimental-to-calculated moment resistance for the same three codes. The axial load ratio is defined as the applied axial force divided by the compressive resistance of the column when no moment is applied. The notation of M_f and M_r is used in these graphs to represent the experimental and theoretical moment resistances, respectively.

Different symbols are used in Figs. 2 and 3 to identify the approach taken to load the specimen in compression/flexure, and to see if any resulting trends could be observed. In type A, the bending moment was produced by applying an eccentric axial load to the column. In the type B columns, two transverse loads were applied close to the middle of the column. A horizontal load was applied in a cyclic manner to the tip of a vertical cantilever for the type C columns. The bending moment for type D columns was produced in the same manner as type B columns but applied in a cyclic manner.

Figs. 2 and 3 show that all code predictions do not appear to be significantly affected by the type of loading methods, and that the equations generally (but not always) become more conservative as the D/t ratio of the steel tube increases. Fig. 3 also shows that the accuracy of the CAN/CSA-S16.1-M94 and Eurocode 4 (1994) equations does not depend on the axial load ratio. However, for AISC LRFD (1994), as the amount of axial load applied on the column increases, so does the ratio of experimental-to-calculated moment resistance, becoming extremely conservative for larger compressive forces.

It is noteworthy that all three codes produced conservative results or slightly unconservative results within the variability expected for this type of calculations. However, all codes produce grossly unconservative results for two of the four class 1 columns that Knowles and Park (1969) tested. Closer examination of Knowles and Park's data did not reveal any peculiar characteristic which would explain the unusually poor comparison between experimental results and theoretical computations for these two columns and the nature of this discrepancy remains unresolved.

Development of Flexural Strength Model

A computer program was written to generate a force–deflection curve from the structural characteristics of a concrete-filled steel tube, using a classic moment–curvature procedure in which the steel tube and the concrete core are divided into layers. The program calculates each layer's individual area, center of gravity, stress, and force corresponding to a given curvature and neutral axis location. Forces from all layers are summed together and the neutral axis is iteratively moved until the sum becomes equal to the applied axial force. The corresponding moment at each curvature is then calculated. Finally, the force is taken as the moment divided by the height of the column and the deflection is calculated by integration of the curvature.

Specimens CFST 64, CFST 34, CFST 42, and CFST 51, tested by Marson and Bruneau (2000) were used to determine the material models that could best predict the experimentally observed behavior using a simple plasticity framework. Actual dimensions of the steel tube and the strengths found from testing the steel coupons and the concrete cylinders were used in the calculations, as well as assumptions that the maximum moment occurs at the concrete foundation, and that the column moment linearly decreases from the top of the concrete foundation to the top steel plate. Strain gauge data reported elsewhere (Marson and Bruneau 2000) confirm that these are reasonable approximations for all of

Table 2. Calculated Strength per Existing Codes and per Proposed Equations

									AISC LRFD		Eurocode 4		CSA-S16.1		Proposal A		Proposal B	
Name	Length mm	D mm	t mm	D/t*Fy	Fy MPa	fc' MPa	Pf (kN)	Mf (kNm)	Mr (kNm)	Mf/Mr	Mr (kNm)	Mf/Mr	Mr (kNm)	Mf/Mr	Mr (kNm)	Mf/Mr	Mr (kNm)	Mf/Mr
Class 1 sections																		
Knowles and Park (1969)																		
13	806.4	88.2	5.842	6039	400	41	554.2	10.7	4.0	2.68	6.0	1.78	8.7	1.24	6.4	1.68	8.7	1.23
14	1411.2	88.2	5.842	6039	400	41	469.1	7.9	4.3	1.81	7.0	1.13	4.0	1.96	4.2	1.88	5.7	1.38
15	806.4	88.2	5.842	6039	400	41	194.8	6.4	13.0	0.50	16.8	0.38	13.3	0.48	13.5	0.48	18.4	0.35
16	1108.8	88.2	5.842	6039	400	41	191.3	5.8	12.8	0.46	16.9	0.34	13.9	0.42	12.9	0.45	17.5	0.33
								AVERAGE		**1.36**		**0.91**		**1.02**		**1.12**		**0.82**
								STANDARD DEVIATION		**0.94**		**0.59**		**0.63**		**0.66**		**0.49**
Class 2 sections																		
Marson(1999)																		
CFST 34	2200	323.9	9.5	17928	415	41	1820	444.0	233.8	1.90	400.6	1.11	254.7	1.74	399.5	1.11	379.8	1.17
Alfawakiri (1997)																		
FA1	1605	152.4	3.4	14792	330	89	400	49.2	20.0	2.46	32.1	1.43	21.3	2.32	46.0	1.07	36.2	1.36
FA2	1605	152.4	3.4	14792	330	72	100	37.3	23.9	1.56	33.4	1.12	21.3	1.75	40.4	0.92	33.7	1.11
FA3	1605	152.4	3.4	14792	330	76	700	49.1	12.6	3.89	38.9	1.26	21.3	2.31	41.6	1.18	34.6	1.42
Furlong (1967)																		
9	914	113.4	3.15	14891	414	29	444.8	11.2	5.4	2.06	10.0	1.12	13.1	0.85	9.1	1.23	11.6	0.97
10	914	113.4	3.15	14891	414	29	400.3	11.9	6.7	1.78	11.9	1.00	13.1	0.90	10.2	1.17	12.9	0.92
11	914	113.4	3.15	14891	414	29	333.6	14.7	8.5	1.72	14.6	1.01	13.1	1.12	11.8	1.24	15.0	0.98
12	914	113.4	3.15	14891	414	29	222.4	15.8	11.6	1.36	18.0	0.88	13.1	1.20	14.5	1.09	17.4	0.91
13	914	113.4	3.15	14891	414	29	111.2	16.1	14.5	1.12	18.7	0.87	13.1	1.23	15.0	1.08	18.1	0.89
19	914	126	2.394	15239	290	35	568.5	8.7	0.5	17.83	4.5	1.95	6.0	1.45	5.5	1.58	5.5	1.60
20	914	126	2.394	15239	290	35	533.8	12.6	1.2	10.57	6.2	2.03	7.5	1.69	6.8	1.85	6.7	1.87
21	914	126	2.394	15239	290	35	400.3	15.8	3.9	4.08	12.6	1.25	8.7	1.82	11.6	1.36	11.4	1.39
22	914	126	2.394	15239	290	35	84.5	15.7	9.8	1.60	14.1	1.11	8.7	1.80	13.7	1.15	14.0	1.12
23	914	126	2.394	15239	290	35	82.3	14.2	9.9	1.44	14.1	1.01	8.7	1.63	13.7	1.04	14.0	1.01
24	914	126	2.394	15239	290	35	345.2	15.7	5.0	3.16	13.5	1.17	8.7	1.81	13.7	1.15	12.3	1.28
25	914	126	2.394	15239	290	35	306.0	16.9	5.8	2.93	14.1	1.20	8.7	1.94	13.7	1.23	13.0	1.30
26	914	126	2.394	15239	290	35	266.9	17.5	6.6	2.67	14.7	1.19	8.7	2.01	13.7	1.28	13.6	1.28
27	914	126	2.394	15239	290	35	260.7	17.4	6.7	2.61	14.8	1.18	8.7	2.00	13.7	1.27	13.7	1.27
28	914	126	2.394	15239	290	35	174.8	16.3	8.4	1.94	15.4	1.06	8.7	1.88	13.7	1.19	14.5	1.12
29	914	126	2.394	15239	290	35	89.0	15.8	9.8	1.61	14.2	1.11	8.7	1.81	13.7	1.15	14.0	1.12
30	914	126	2.394	15239	290	35	43.6	14.6	10.2	1.43	13.5	1.08	8.7	1.67	13.7	1.07	13.8	1.06
								AVERAGE		**3.32**		**1.20**		**1.66**		**1.21**		**1.20**
								STANDARD DEVIATION		**3.79**		**0.29**		**0.40**		**0.19**		**0.24**
Class 3 sections																		
Marson(1999)																		
CFST 42	2200	406.4	9.5	21603	505	35	1820	928.0	681.5	1.36	914.8	1.01	608.1	1.53	739.3	1.26	896.6	1.04
								AVERAGE		**1.36**		**1.01**		**1.53**		**1.26**		**1.04**
								STANDARD DEVIATION		**0.00**		**0.00**		**0.00**		**0.00**		**0.00**
Class 4 sections Permitted by Clause 18.6																		
Marson(1999)																		
CFST 51	2200	323.9	6.5	23563	400	35	1600	356.0	158.2	2.25	302.2	1.18	182.3	1.95	289.0	1.23	284.0	1.25
								AVERAGE		**2.25**		**1.18**		**1.95**		**1.23**		**1.25**
								STANDARD DEVIATION		**0.00**		**0.00**		**0.00**		**0.00**		**0.00**
Class 4																		
Marson(1999)																		
CFST 64	2200	406.4	6.5	27635	442	37	1000	591.0	361.8	1.64	522.0	1.13	314.3	1.88	540.2	1.09	518.5	1.14
Knowles and Park (1969)																		
17	806.4	82.55	1.397	28541	483	41	167.9	3.3	2.4	1.39	5.4	0.61	3.8	0.87	356.0	0.01	4.8	0.69
18	806.4	82.55	1.397	28541	483	41	89	2.6	3.6	0.72	6.1	0.43	3.8	0.69	5.1	0.51	5.6	0.47
Prion and Boehme (1994)																		
BP16	2120	152	1.65	30216	328	92	0	21.0	12.2	1.72	17.3	1.21	10.9	1.93	37.5	0.56	17.1	1.23
B11	2120	152	1.65	30216	328	92	470	29.7	8.8	3.39	27.4	1.08	10.9	2.74	37.5	0.79	20.0	1.48
B12	2120	152	1.65	30216	328	92	570	32.1	7.7	4.17	28.2	1.14	10.9	2.96	37.5	0.85	20.7	1.55
B13	2120	152	1.65	30216	328	92	670	28.5	6.6	4.29	28.9	0.99	10.9	2.63	37.5	0.76	21.3	1.34
B14	2120	152	1.65	30216	328	92	820	29.2	5.0	5.79	29.0	1.01	10.9	2.69	37.5	0.78	21.1	1.38
B15	2120	152	1.65	30216	328	92	970	30.5	3.4	8.85	22.5	1.35	10.9	2.81	37.5	0.81	14.4	2.11
B17	2120	152	1.65	30216	328	92	270	30.1	10.9	2.76	24.1	1.25	10.9	2.77	37.5	0.80	18.8	1.60
BP18	2120	152	1.65	30216	328	92	270	30.8	11.0	2.83	24.1	1.28	10.9	2.84	37.5	0.82	18.8	1.64
BP19	2120	152	1.65	30216	328	92	670	34.8	6.6	5.24	28.9	1.20	10.9	3.21	37.5	0.93	21.3	1.64
BP20	1071	152	1.65	30216	328	92	1273	21.4	2.3	9.40	21.9	0.98	10.0	2.13	37.5	0.57	17.3	1.24
BP21	1071	152	1.65	30216	328	92	1451	13.8	0.7	20.60	16.6	0.83	10.0	1.38	37.5	0.37	11.6	1.19
BP22	1071	152	1.65	30216	328	92	1309	15.9	2.0	8.15	20.8	0.76	10.0	1.59	37.5	0.42	16.1	0.99
Furlong (1967)																		
14	914	151.2	1.5372	32549	331	26	567.6	9.9	0.8	13.09	6.6	1.50	8.1	1.21	7.8	1.26	7.2	1.38
15	914	151.2	1.5372	32549	331	26	421.7	17.7	3.9	4.58	14.4	1.23	9.2	1.91	14.5	1.22	12.9	1.37
16	914	151.2	1.5372	32549	331	26	286.0	17.1	6.7	2.54	17.1	1.00	9.2	1.85	15.8	1.08	15.9	1.08
17	914	151.2	1.5372	32549	331	21	136.1	16.1	9.6	1.68	16.3	0.99	9.2	1.74	14.3	1.12	15.7	1.02
18	914	151.2	1.5372	32549	331	21	135.2	14.9	9.6	1.56	16.3	0.92	9.2	1.62	14.3	1.04	15.7	0.95
								AVERAGE		**5.22**		**1.04**		**2.07**		**0.79**		**1.27**
								STANDARD DEVIATION		**4.74**		**0.25**		**0.71**		**0.31**		**0.36**

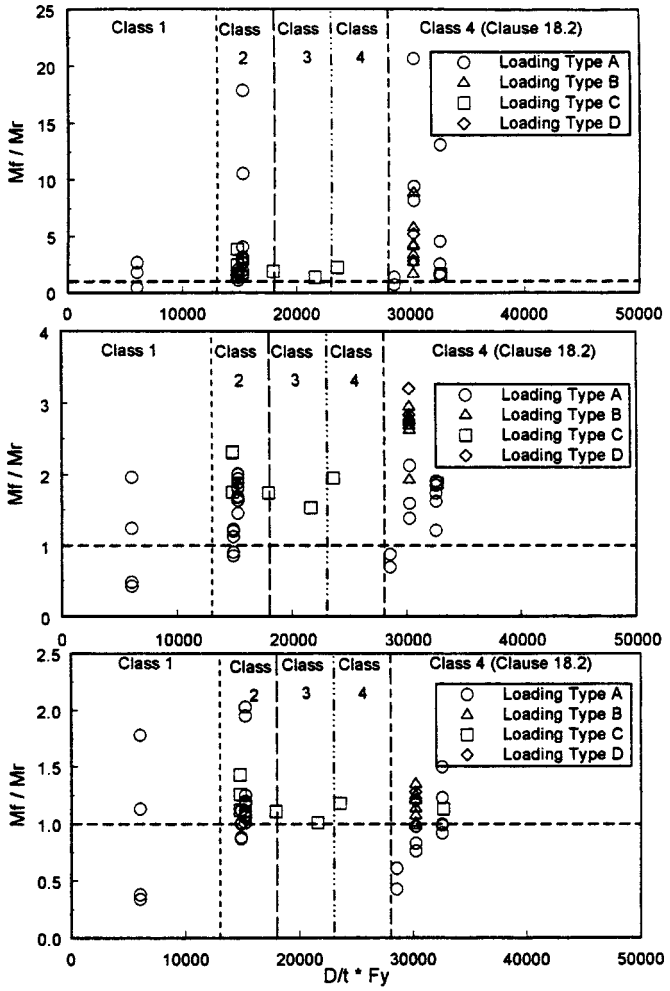

Fig. 2. Ratio of experimental-to-predicted strengths as a function of D/t ratio calculated using: (a) AISC LRFD (1994); (b) CAN/CSA-S16.1-M94; and (c) Eurocode 4 (1994)

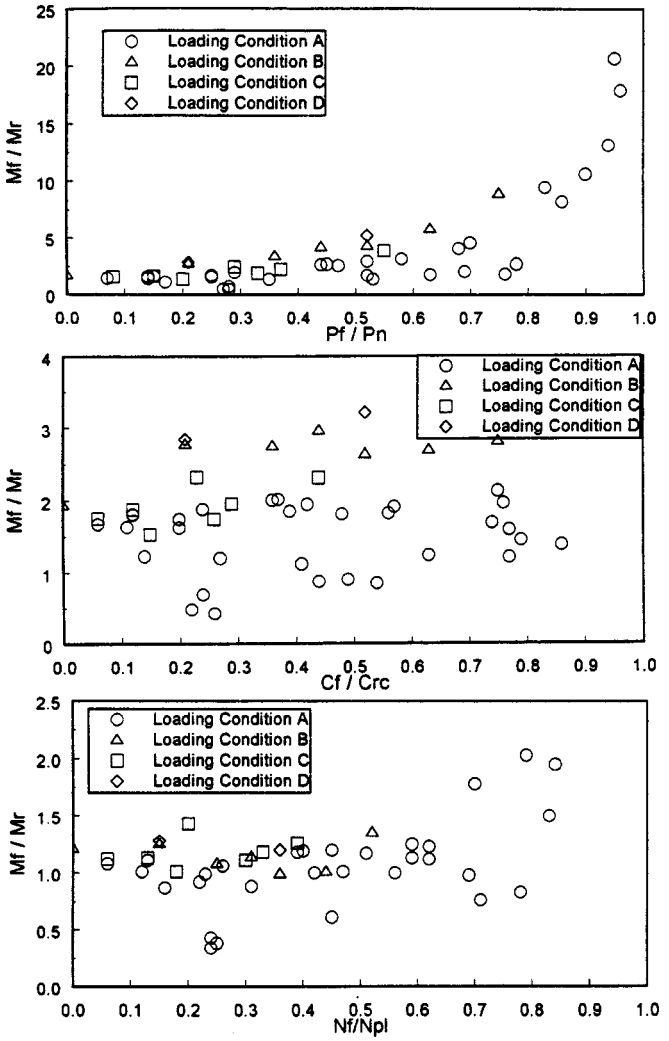

Fig. 3. Ratio of experimental-to-predicted strengths as a function of ratio of applied axial force to plastic squash load, calculated using: (a) AISC LRFD (1994); (b) CAN/CSA-S16.1-M94; and (c) Eurocode 4 (1994)

the specimens tested. Steel was modeled by a bilinear stress–strain relationship. Seven concrete axial compression stress–strain models were considered: model 1, confined concrete model (Mander et al. 1988); model 2, unconfined concrete model (Hognestad 1951); model 3, confined concrete model (Saaticuglu and Ravzi 1992); model 4, unconfined concrete model with high ductility; model 5, unconfined concrete model with CISC provisions; model 6, unconfined concrete model with high ductility and CISC provisions; and model 7, equivalent to model 1 but with arbitrarily reduced confined concrete strengths.

A detailed description of each model and the rationale that led to their consideration is presented in Marson and Bruneau (2000). Fig. 4 shows the resulting force–tip displacement curves for the first six models. Results show that increases of concrete strength beyond f'_c due to confinement (such as proposed by Mander et al. 1988 and Saaticuglu and Ravzi 1992) overestimate the strength of concrete-filled tubes. However, use of an unconfined concrete model such as the one proposed by Hognestad (1951) is too conservative. Reasonably accurate results are obtained with model 4, which assumes that the steel tube confines the concrete core in such a way that the strength of the concrete is f'_c, instead of the usual concrete column strength of $0.85f'_c$, and that this strength can be sustained up to large ductilities. This is essentially an elastic perfectly plastic concrete model, with the plastic portion of the curve assumed to result from the steel tube providing confinement to the concrete core. The strength predicted by this model still slightly conservatively underestimates actual strength, giving 0.92, 0.92, 0.99, and 0.87 of the experimentally obtained strengths for specimens CFST 64, CFST 34, CFST 42, and CFST 51, respectively.

Consideration of this unconfined concrete model with high ductility, along with the CAN/CSA-S16.1-M94 equations that increase the concrete strength of a composite column to account for a moderate level of confinement (model 5), lead to slightly lower strengths. It was observed in that case that the additional concrete strength gained by confinement was offset by the decrease in steel strength due to biaxial stresses.

Proposed New Design Equations

In the following, new equations are proposed to calculate the strength of circular concrete-filled steel tube beam columns with better results than by the current North American codes. These equations are formulated in a format compatible with the Cana-

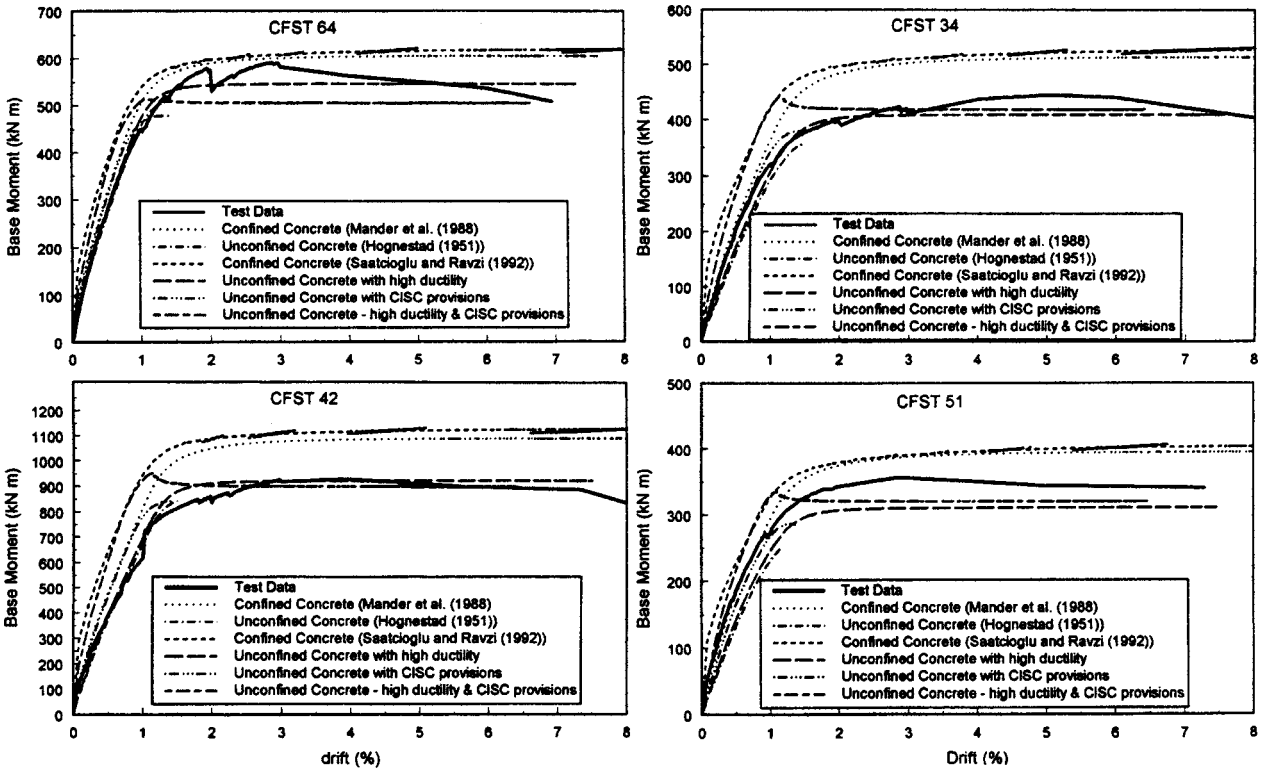

Fig. 4. Comparison of moment–drift curves experimentally obtained for specimens CFST 64, 51, 42, and 34, with results predicted using various models

dian S16.1 and American AISC codes (except that F_y and f'_c would be replaced by ϕF_y and $\phi_c f'_c$ in code implementations).

Flexural Strength

The flexural strength of a concrete-filled pipe is calculated using the equilibrium diagram shown in Fig. 5. The following equations define the forces acting on the composite section:

$$T_r = A_{st} F_y \tag{1}$$

$$T_r = T_{max} - C_r \tag{2}$$

$$T_r = C_r + C'_r \tag{3}$$

$$T_{max} = A_s F_y \tag{4}$$

where T_r=tensile force in the steel tube; A_{st}=area of tensile steel; F_y=yield strength of the steel tube; T_{max}=total force if all steel is in tension; C_r=axial compressive resistance of the steel tube; C'_r=axial compressive resistance of the compressed concrete core; and A_s=total area of steel. To solve for the neutral axis location, *h*, in Fig. 5, the above four equations are combined to produce one equation

$$2A_{st}F_y = A_s F_y + C'_r \tag{5}$$

The terms in the above equation are defined below

$$A_{st} = (2\pi R - m)t = (\pi D - m)t \tag{6}$$

$$m = \beta R \tag{7}$$

$$A_s = 2\pi Rt = \pi Dt \tag{8}$$

$$C'_r = A_{conc} f'_c = \left[\frac{mD}{4} - \frac{c(R-a)}{2}\right] f'_c = \left[\frac{\beta D^2}{8} - \frac{b_c}{2}\left(\frac{D}{2} - a\right)\right] fc' \tag{9}$$

$$a = \frac{b_c}{2}\tan\left(\frac{\beta}{4}\right) \tag{10}$$

$$c = D\sin\left(\frac{\beta}{2}\right) \tag{11}$$

where *m*=arc length of the tube in compression; β=angle in radians from the center of the tube; and sustaining the arc *m*, *R*, and *D*=radius and diameter of the steel tube, respectively (Fig. 5). Substituting these terms into Eq. (5), and expressing in terms of β, the equation becomes

$$\beta = \frac{A_s F_y + 0.25D^2 f'_c[\sin(\beta/2) - \sin^2(\beta/2)\tan(\beta/4)]}{(0.125D^2 f'_c + DtF_y)} \tag{12}$$

There is no closed form solution for the above equation so an iterative solution is required to obtain β. Once the value for β is

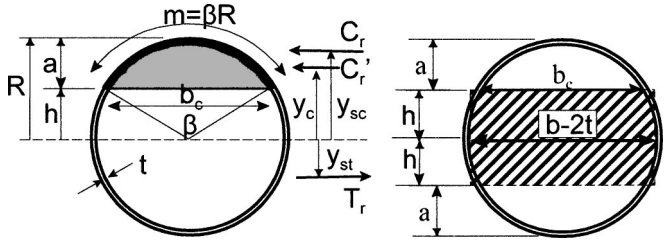

Fig. 5. Free-body diagrams used to develop flexural strength equations

found, C_r, C_r', and T_s can be calculated. The distances from the neutral axis for C_r, C_r', and T_s, are y_{sc}, y_c, and y_{st}, respectively, where

$$y_{sc}=\frac{Rb_c}{m} \tag{13}$$

$$y_c=\frac{b_c^3}{6[Rm-b_c(R-a)]} \tag{14}$$

$$y_{st}=\frac{Rb_c}{2\pi R-m} \tag{15}$$

From simple statics, M_{rc} is defined as

$$M_{rc}=C_r e+C_r' e' \tag{16}$$

$$e=y_{st}+y_{sc}=b_c\left[\frac{1}{(2\pi-\beta)}+\frac{1}{\beta}\right] \tag{17}$$

$$e'=y_{st}+y_c=b_c\left[\frac{1}{(2\pi-\beta)}+\frac{b_c^2}{1.5\beta D^2-6b_c(0.5D-a)}\right] \tag{18}$$

Alternatively, using an approximate geometry method, in which the contribution of a rectangular central section of height $2h$ is subtracted from the plastic moment of the entire section (Fig. 5), a closed-form solution is possible and a conservative value of M_{rc} is directly given by

$$M_{rc}=(Z-2th_n^2)Fy+\left[\tfrac{2}{5}(0.5D-t)^3-(0.5D-t)h_n^2\right]f_c' \tag{19}$$

where

$$h_n=\frac{A_c f_c'}{2Df_c'+4t(2F_y-f_c')} \tag{20}$$

and Z=plastic modulus of the steel section alone.

For capacity design purposes, in determining the force to consider for the design of capacity protected elements, it is recommended to increase the moment calculated by this approximate method by 10%.

CSA-S16.1 Interaction Curve for Axial and Flexural Resistance

Availability of the above equations for M_{rc} for circular concrete-filled steel tubes makes it possible to calculate the moment resistance of these composite columns with CAN/CSA-S16.1-94 using the following interaction equation:

$$\frac{C_f}{C_{rc}}+\frac{B\omega_1 M_f}{M_{rc}\left(1-\dfrac{C_f}{C_{ec}}\right)}=1.0 \tag{21}$$

where C_f=applied axial force on the column, and C_{rc}=axial resistance of a concrete column as defined in the Appendix. M_f=applied moment on the column; C_{ec}=Euler buckling strength of a concrete-filled steel tube, and B is defined as

$$B=\frac{C_{rco}-C_{rcm}}{C_{rco}}=1-\frac{C_{rcm}}{C_{rco}} \tag{22}$$

where C_{rco}=compressive resistance as calculated in the Appendix with $\lambda=0$, and C_{rcm} is the compressive resistance of the concrete core alone with no slenderness effect taken into account. As seen in Fig. 6, the moment capacity with no axial force applied and a neutral axis location of h above the center of gravity is the same moment capacity as for an axial force equal to C_{rcm} and a neutral axis location of h below the center of gravity. As seen in the equations in Fig. 6, M_{rc} is equal to M_{rcm}.

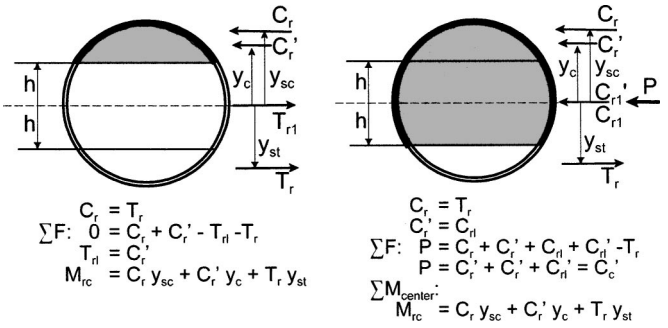

Fig. 6. Free-body diagrams used as a step to develop axial and flexural interaction diagram

Fig. 7 shows the effect of B for values of B equal to 1.0, 0.85, 0.75, and 0.5. CAN/CSA-S16.1 states that $B=1.0$ can conservatively be used, but, as shown on Fig. 7, this can be grossly conservative. The factor B changes a straight line interaction curve into a bilinear interaction curve. As B decreases, a column can resist more axial force in addition to resisting its full plastic moment. For a column, in which $\lambda\neq 0$, the interaction curve is automatically adjusted downward by the ratio C_f/C_{rc}. In that case, the greatest axial force that can be resisted in addition to the full moment is C_{rcm} reduced by the ratio C_{rc}/C_{rco}.

The interaction curve using this procedure for the four specimens tested by Marson and Bruneau (2004) is shown in Fig. 1 as CAN/CSA-S16.1-99 (proposal A). For this interaction curve, the experimental-to-calculated ratios are 1.20, 1.15, 1.02, and 1.28 for specimens CFST 64, CFST 34, CFST 42, and CFST 51, respectively, a much better agreement with experimental results than provided by the existing CAN/CSA-S16.1-94. Table 2 shows a comparison between results obtained with CAN/S16.1-M94 and the new proposed equation (proposal A), with previous research data. Improvements in the average and standard deviation of the experimental to calculated strength are significant. The standard deviation of the experimental to calculated moment resistance is 0.64 and 0.37, and the average is 1.79 and 1.03, for CAN/S16.1-M94 and proposal A, respectively.

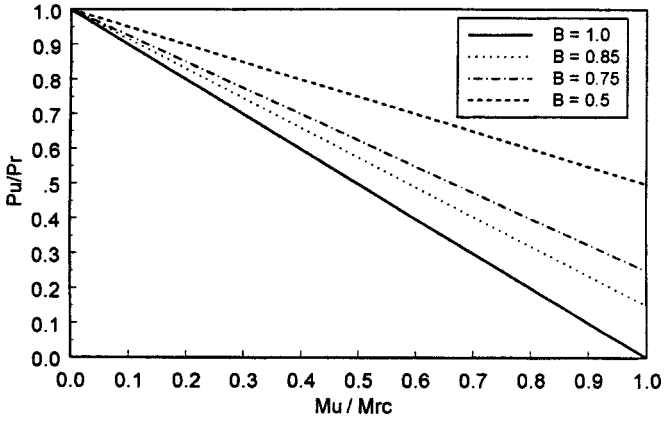

Fig. 7. Effect of B on shape of CSA-S16.1 interaction diagram

Proposed New Equations for AISC LRFD Provisions

Similar equations have been developed in a format compatible with both the AISC LRFD Provisions and AASHTO LRFD specifications. As such, concrete-filled steel pipe members required to resist both axial compression and flexure and intended to be ductile substructure elements must be proportioned so that

$$\frac{P_u}{P_r}+\frac{BM_u}{M_{rc}}\leqslant 1.0 \tag{23}$$

and

$$\frac{M_u}{M_{rc}}\leqslant 1.0 \tag{24}$$

where P_r=defined as currently done by these respective code documents, and

$$B=\frac{P_{ro}-P_{rc}}{P_{rc}}, \tag{25}$$

where P_{ro}=factored compressive resistance per AISC or AASHTO (with $\lambda=0$); $P_{rc}=\phi_c A_c f'_{c'}$; and M_u=maximum resultant moment applied to the member in any direction (again, a conventional parameter for which strength equations are given in AISC and AASTHO).

In this case, the factored moment resistance of a concrete filled steel pipe is also given by Eqs. (16)–(20). Although not presented here due to space constraints, tabulated data, again, show significant improvements when compared against past research results, with average and standard deviation of the ratio of experimental-to-calculated value of 1.38 and 0.80, respectively.

Conclusion

A new proposed design axial-flexure interaction equation appears to predict reasonably well the behavior of concrete-filled steel pipes. The proposed design equations produce axial–flexure interaction equations in much better agreement with the existing data than the equations for circular concrete-filled steel tubes currently used by the Canadian CAN/CSA-S16.1-M94 standard, or American AISC LRFD 1994 specifications. The new model used a concrete model able to develop f'_c up to high ductilility (caused by the confinement of the steel tube) and a bilinear stress–strain model for the steel tube. Good correlation is obtained between predicted strength and experimental data for the results of tests by Marson and Bruneau (2004) as well as tests by other researchers. On the basis of the results presented here, this model has already been implemented in the 2001 edition of the CSA-S16-01 ''limit state design of steel structures'' (CSA 2001) and in the ''recommended LRFD guidelines for the seismic design of highway bridges'' (MCEER/ATC 2003).

Acknowledgments

This research program was funded by the Natural Science and Engineering Research Council of Canada and the Structural Steel Education Foundation. This support is sincerely appreciated. However, the opinions expressed in this paper are those of the writers and do not reflect the views of the aforementioned sponsors.

Appendix. Summary of Design Provisions for Concrete-Filled Circular Steel Tube

AISC LRFD

For a concrete-filled tube to qualify as a composite column, according to the AISC code, the following limits must be satisfied:

- The steel pipe cross section must be at least 4% of the gross total column cross-sectional area.
- The specified concrete strength must be between 20 and 55 MPa—the lower limit to ensure a minimum degree of quality control, the upper limit because AISC believes that an insufficient number of tests have been performed on composite columns built with high strength concrete.
- The minimum wall thickness of the steel member, to prevent local buckling before yielding, shall be $D\sqrt{F_y/8E_s}$, where D is the diameter of the circular steel shell, E_s is the modulus of elasticity of steel, and F_y is the steel yield stress.

Axial Compression

Compressive strength calculations for concrete-filled steel columns are the same as for bare steel structural members in AISC (1986) with the exception that the modified properties F_{my}, E_m, and r_m are used. The axial design strength, P_n, is calculated as

$$\phi_c P_n=0.85A_s F_{\rm cr} \tag{26}$$

where 0.85=value of the resistance factor for compression, ϕ_c, and the critical column stress, $F_{\rm cr}$ is

$$F_{\rm cr}=(0.658^{\lambda_c^2})F_{my} \quad \text{for } \lambda_c^2\leqslant 2.25$$

$$F_{\rm cr}=\frac{0.877}{\lambda_c^2}F_{my} \quad \text{for } \lambda_c^2>2.25 \tag{27}$$

$$\lambda_c^2=\left(\frac{KL}{\pi r_m}\right)^2\frac{F_{my}}{E_m}$$

where r_m=modified radius of gyration about the axis of buckling. The modified yield stress, F_{my}, and the modified modulus of elasticity, E_m are defined as:

$$F_{my}=F_y+\frac{c_2 f'_c A_c}{A_s}$$

$$E_m=E_s+\frac{c_3 E_c A_c}{A_s} \tag{28}$$

where c_2=coefficient equal to 0.85 because the confined concrete inside a tube can reach stresses as high as $0.85*f'_c$, and c_3=coefficient equal to 0.4 that accounts for uncertainty in the concrete contribution to the buckling strength of a composite concrete-filled tube. Note that for $\lambda=0$, the strength equation becomes

$$\phi P_n=0.85[A_s F_y+0.85A_c f'_c] \tag{29}$$

which means that the capacity of a concrete-filled steel column is taken as the sum of the strengths of its parts. AISC also states that the conventional calculation of the radius of gyration cannot be used in a concrete-filled steel column because, although both the steel and the concrete contribute to the flexural deformation of the cross section, either steel or concrete may dominate flexural stiffness, depending on cross-section width and thickness. There is no

single equation that can reliably be used to account for the composite flexural stiffness. Therefore, the AISC indicates that if the steel predominates, the radius of gyration of steel is adequate for the entire section, however, if the flexural deformation is resisted primarily by the concrete, the radius of gyration of concrete is adequate for the section. Consequently, AISC specifies that r_m should be taken as the radius of gyration of the steel tube alone, but no less than 30% of the thickness of gross composite section in the plane of buckling.

Bending and Axial Load

For symmetrical composite columns about the plane of bending, the interaction of compression and flexure should be limited by

$$\frac{P_u}{\phi_c P_n}+\frac{8M_u}{9\phi_b M_n}\leqslant 1.0 \quad \text{for } P_u \geqslant 0.2\phi_c P_n$$
$$\frac{P_u}{2\phi_c P_n}+\frac{M_u}{\phi_b M_n}\leqslant 1.0 \quad \text{for } P_u < 0.2\phi_c P_n \tag{30}$$

where P_u=factored axial force; M_u=factored moment increased for member and global slenderness effects; the axial design strength, $\phi_c P_n$, is defined above; and ϕ_b=resistance factor for bending, taken equal to 0.85. The AISC specifications states that the specified flexural design strength be computed using the plastic strength distribution on the cross section, and requires an empirical reduction of that value in absence of shear connectors when $P_u/\phi P_n$ is less than 0.3.

CAN/CSA-S16.1-M94

According to the Canadian Standard CAN/CSA-S16.1-M94 ''limit states design of steel structures,'' hollow structural sections (HSS) classified as classes 1, 2, and 3, and completely filled with concrete may be used as composite columns to carry axial loads. Class 4 sections completely filled with concrete may also be designed as composite columns if outside diameter-to-thickness ratios of circular HSS is less than $28{,}000/F_y$.

Axial Compression

CAN/CSA-S16.1-M94 expresses the factored compressive resistance, C_{rc} of concrete-filled columns as

$$C_{rc}=\tau C_r+\tau' C_r' \tag{31a}$$

$$C_r'=0.85\phi_c f_c' A_c \lambda_c^{-2}[\sqrt{1+0.25\lambda_c^{-4}}-0.5\lambda_c^{-2}] \tag{31b}$$

$$\lambda_c=\frac{kL}{r_c}\sqrt{\frac{f_c'}{\pi^2 E_c}} \tag{31c}$$

$$C_r=\phi A_s F_y(1+\lambda_s^{2n})^{(-1/n)} \tag{31d}$$

$$\lambda_s=\frac{kL}{r_s}\sqrt{\frac{F_y}{\pi^2 E_s}} \tag{31e}$$

where τ=coefficient used to reduce the contribution of the steel due to biaxial stresses generated to create concrete confinement, and τ'=coefficient that increases the contribution of the concrete for the same reason. For circular hollow structural sections with a height-to-diameter ratio of 25 or greater, CAN/CSA-S16.1-M94 specifies, $\tau=\tau'=1.0$ (which implies no effective confinement). Otherwise,

$$\tau=\frac{1}{\sqrt{1+\rho_s+\rho_s^2}}$$
$$\tau'=1+\left(\frac{25\rho_s^2\tau}{(D/t)}\right)\left(\frac{F_y}{0.85f_c'}\right) \tag{32}$$
$$\rho_s=0.02\left(25-\frac{L}{D}\right)$$

Combined Bending and Axial Load

CAN/CSA-S16.1-94 has two methods for the design of composite columns. In a first method, the moment resistance of the composite section is considered in calculations. However, use of this method is only permitted for rectangular concrete-filled steel tube (CFST) sections. This method depends on the calculation of the moment resistance of a composite section, M_{rc}, which is only given for rectangular sections (because the research in support of these equations was performed for rectangular sections only). An example on how to calculate the moment resistance for rectangular CFST sections is documented in Picard and Beaulieu (1997). The second calculation method presented in CAN/CSA-S16.1-94, by default the only method permissible for circular concrete-filled steel tubes, assumes that bending is resisted by the steel section alone. This more conservative method (used in Fig. 1) severely underestimates the moment capacity of beam columns when the applied axial force is less than the compressive resistance from the concrete core alone. Since the steel section is assumed to resist all bending forces, the steel shell must be designed as a beam-column to resist all flexure, plus the axial compression load equal to the difference between the total axial compression load applied, C_f, and the portion that is resisted by the concrete core, $\tau' C_r'$. Therefore, when $M_f \leqslant \tau M_r$ and $C_f > \tau' C_r'$.

$$\frac{C_f-\tau' C_r'}{\tau C_r}+\frac{\omega_1 M_f}{\tau M_r\left(1-\dfrac{C_f-\tau' C_r'}{C_e}\right)}\leqslant 1.0 \tag{33}$$

where M_f=factored applied moment; C_e=Euler buckling strength of the steel tube alone; and ω_1=equivalent uniform bending effect in beam columns (taken as 1.0 for all cases considered in this paper, in accordance with the CSA standard). M_r=factored moment resistance equal to $\phi_s Z F_y$ for classes 1 and 2 sections, and $\phi_s S F_y$ for class 3 sections. The resistance factor for steel, ϕ_s, is equal to 0.9, and for concrete, ϕ_c, equals 0.6.

Eurocode 4

Eurocode 4 (1994)—''design of composite steel and concrete structures,'' limits its scope to concrete-filled steel tubes for which:

- The steel contribution ratio, δ, must be between 0.2 and 0.9, where
$$\delta=\frac{(A_a f_y)/\gamma_{Ma}}{N_p}$$
and A_a=cross-sectional area of the steel tube; γ_a=partial safety factor for steel taken equal to 1.10; and N_p=plastic compressive resistance of the composite column.
- The nondimensional slenderness factor, $\lambda=\sqrt{N_p/N_{cr}}$, must not exceed 2.0, where N_{cr}=Euler buckling load, and N_p=plastic strength, both defined below.

- The diameter-to-thickness ratio is limited by $d/t \leq 90(235/f_y)$.

Axial Compression

The plastic axial resistance, N_p of a circular concrete-filled steel column is given as

$$N_p = \frac{A_a \eta_2 f_y}{\gamma_{Ma}} + \frac{A_c f_{ck}}{\gamma_c} * \left[1 + \eta_1 \left(\frac{t}{d}\right)\left(\frac{f_y}{f_{ck}}\right)\right] \tag{34}$$

where A_c=cross-sectional area of the concrete core; γ_{Ma} and γ_c=partial safety factors for steel and concrete $f_{ck} \equiv f_c'$; and where η_1 and η_2=values that, respectively, increase the concrete strength due to confinement and reduce steel strength due to biaxial stresses when λ is no greater than 0.5 and M_f is no greater than $N_f(d/10)$, where M_f and N_f are the applied moment and axial load, respectively.

The member is determined to have sufficient resistance if $N_f \leq \chi N_P$, where

$$\chi = f_k - \sqrt{(f_k^2 - \lambda^{-2})} \leq 1.0$$
$$f_k = 0.5\lambda^{-2}[1 + 0.21(\lambda - 0.2) + \lambda^2] \tag{35}$$

N_{cr}=elastic critical load used to calculate the slenderness factor, and is given by

$$N_{cr} = \frac{\pi^2 (EI)_e}{L^2} \tag{36}$$

where L=buckling length, and $(EI)_e$=equivalent elastic modulus of the composite column calculated as the sum of the individual components

$$(EI)_e = E_a I_a + 0.8 E_{cd} I_c \tag{37}$$

where I_a and I_c=second moments of area for the steel and uncracked concrete core, respectively; E_a=elastic modulus for the structural steel taken as 210,000 MPa; and E_{cd}=secant modulus of elasticity for short term loading of concrete.

Bending and Axial Load

The code uses a simplified force versus moment interaction diagram to calculate the resistance of a section in combined bending and axial loading. Plastic analysis and a rectangular stress block for the steel tube and concrete core are used to derive the equations. Interaction diagram is built using four points: point A ($N_A = N_P$ and $M_A = 0$) represents the case of zero moment and full plastic axial load; point C (N_C and M_C), corresponds to the compressive resistance of the concrete core; point D (N_D and M_D) is calculated as half of the axial resistance at point C; point B (N_B and M_B), corresponds to the plastic moment in the absence of axial force applied ($M_B = M_P$), therefore, N_B is equal to zero. Bending moment resistance are defined as

$$M_A = 0$$
$$M_D = Z_s \frac{f_y}{\gamma_{Ma}} + 0.5 * Z_c \frac{f_{ck}}{\gamma_c} \tag{38}$$
$$M_B = M_C = M_D - 2(t * h_n^2)\frac{f_y}{\gamma_{Ma}} - 0.5((D - 2t) * h_n^2)\frac{f_{ck}}{\gamma_c}$$

where

$$h_n = \frac{N_C}{(2Df_{ck} + 4t(2f_y - f_{ck}))}$$

where Z_s and Z_c=plastic section moduli of the steel tube and concrete core, respectively, and D and t=outside diameter and thickness of the steel tube, respectively. Strength obtained from the interaction diagram are then reduced to account for slenderness and imperfections, using the factors χ_n and χ_d

$$\chi_d = \frac{N_f}{N_p}$$
$$\chi_n = \chi * 0.25 * (1 - r) \quad \text{but} \quad \chi_n \leq \chi_d \tag{39}$$

where r=ratio of the lesser to the greater end moments. The corresponding bending moment resistance, μ_k and μ_d are determined from the respective axial resistance factor, χ and χ_d. The length of μ is calculated as

$$\mu = \mu_d - \mu_k * \frac{\chi_d - \chi_n}{\chi - \chi_n} \tag{40}$$

Graphically, the concept can be illustrated by constructing a nondimensional interaction diagram, with a shaded triangular region on the left of the diagram (along the axial force axis) and sized as a function of the slenderness factor. For a given axial load applied, the length from the right side of that triangle to the right edge of the interaction diagram gives the usable moment resistance.

Therefore, the member flexural resistance is given by the following equation:

$$M_f \leq 0.9 \mu M_p \tag{41}$$

where M_f=maximum design bending moment within the column length. However, for all calculations presented in this paper, member resistance is calculated neglecting the 0.9 factor as it appears to be another safety factor.

References

Alfawakiri, F. (1997). ''Behavior of high strength concrete-filled circular steel tube beam columns.'' MS thesis, Univ. of Ottawa, Ottawa.

American Association of State Highway and Transportation Officials (AASHTO). (1994). ''LRFD bridge design specifications.'' Washington, D.C.

American Concrete Institution (ACI). (1963). ''Standard building code requirements for reinforced concrete.'' *ACI 318-63*, Detroit.

American Institute of Steel Construction (AISC). (1986). *Load and resistance factor design—Manual of steel construction*. 1st Ed., Chicago.

American Institute of Steel Construction (AISC). (1994). *Load and resistance factor design—Manual of steel construction*. 2nd Ed., Chicago.

Canadian Standards Association (CSA). (1988). ''Standard for the design of highway bridges—CAN/CSA-S6-88.'' Rexdale Ont., Canada.

Canadian Standards Association (CSA). (1994). ''Limit states design of steel structures—CAN/CSA-S16.1-94.'' Rexdale, Ont., Canada.

Canadian Standards Association (CSA). (2001). ''Limit states design of steel structures—CAN/CSA-S16-01.'' Rexdale, Ont., Canada.

Furlong, R. W. (1967). ''Strength of steel-encased concrete beam columns.'' *J. Struct. Div. ASCE*, 93, 113–124.

Hognestad, E. (1951). ''A study of combined bending and axial load in reinforced concrete members.'' *Bulletin Series No. 399*, Univ. Illinois Eng., Experimental Station, Urbana, Ill.

Knowles, R. B., and Park, R. (1969). ''Strength of concrete-filled steel tubular columns.'' *J. Struct. Div. ASCE*, ST12, 2565–2586.

Mander, J., Priestley, M., and Park, R. (1988). ''Observed stress–strain behavior of confined concrete.'' *J. Struct. Eng.*, 114(8), 1827–1849.

Marson, J., and Bruneau, M. (2004). ''Cyclic testing of concrete-filled circular steel bridge piers having encased fixed-based detail.'' *J. Bridge Eng.*, 9(1), 14–23.

Marson, J., and Bruneau, M. (2000). ''Cyclic testing of concrete-filled

circular steel bridge piers having encased fixed-based detail.'' *Ottawa Carleton Earthquake Eng. Res. Center, Rep. No. OCEERC 00-22*, Univ. of Ottawa, Ottawa.
MTO. (1991). *Ontario highway bridge design code*, 3rd Ed., Ministry of Transportation, Government of Ontario, St. Catherines Ont., Canada.
MCEER/ATC. (2003). ''Recommended LRFD guidelines for the seismic design of highway bridges.'' *Multidisciplinary Center for Earthquake Eng. Res. and Applied Technology Council Joint Venture, Rep. No. ATC/MCEER-49*, Buffalo, N.Y.
Picard, A., and Beaulieu, D. (1997). ''Resistance of concrete-filled hollow structural sections.'' *Can. J. Civ. Eng.*, 24, 785–789.
Prion, H., and Boehme, J. (1994). ''Beam-column behavior of steel tubes filled with high strength concrete.'' *Can. J. Civ. Eng.*, 21(2), 207–218.
Saatcioglu, M., and Razvi, S. R. (1992). ''Strength and ductility of confined concrete.'' *J. Struct. Eng.*, 118(6), 1590–1607.
Viest, I. M., Colaco, J. P., Furlong, R. W., Griffis, L. G., Leon, R. T., and Wyllie, L. A., Jr. (1997). *Composite construction design for buildings*, American Society of Civil Engineers and McGraw-Hill, New York.